

Optimal Industrial Load Control in Smart Grid: A Case Study for Oil Refineries

Armen Gholian, Hamed Mohsenian-Rad, Yingbo Hua

Department of Electrical Engineering

University of California, Riverside

Riverside, CA, USA

armen.gholian@email.ucr.edu, {hamed, yhua}@ee.ucr.edu

Joe Qin

Department of Chemical Engineering & Material Sci.

University of Southern California

Los Angeles, CA, USA

sqin@usc.edu

Abstract—The current literature on optimal load control is mainly focused on residential and commercial load sectors. In this paper, we investigate optimal load control for industrial load which involves several new and distinct research challenges. For example, while most residential appliances operate independently, industrial units are highly *inter-dependent* and must follow a certain operational sequence. This is particularly the case in industries that involve process control: each unit can start operation only if its feeding units finish their operations. Considering an oil refinery industry as an example, we not only identify some of the most important operational sequences in this particular industry, but also develop mathematical models that can help us integrate the identified operational sequences in an optimization-based industrial load control framework. We assess the performance of our design through various simulations.

Index Terms—Demand response, load management, manufacturing industries, oil refineries, optimal scheduling.

I. INTRODUCTION

The global demand for electricity has increased by 2.3% per year since 2008 and this trend is expected to continue [1]. To assure reliable service, generation capacity is designed to match the *peak demand*. Thus, it is desirable to reduce the peak-to-average ratio in load profile in each region to minimize the need to build new power plants. This can be achieved by a combination of *smart pricing* by utilities and *optimal load control* by consumers such that we can utilize any *controllable load* in each load sector to not only reduce the peak demand but also help users reduce their energy expenditure.

Most prior work on optimal load control has mainly focused on residential and commercial loads [2]–[4]. However, since over 40% of world’s generated electricity is consumed by industries [5], addressing industrial load control is also necessary to reduce the peak demand more effectively. Of course, the exact load profiles and potential for load control can vary among industries, for example, depending on whether the industry is a manufacturing unit (e.g., automotive, food, pulp-and-paper, chemicals, refining, and iron and steel) or non-manufacturing unit (agriculture, mining, and construction). Our focus in this paper is on manufacturing load control.

A common characteristic that makes industrial load control different from residential load control is the typical *inter-dependency* among industrial units that belong to the same product chain, whether a car assembly line or an oil refinery: a unit cannot start its operation unless its feeding units produce its feed. Clearly, this is not the case in residential loads

where appliances operate independently. For example, it is not necessary to start and finish the charging of an electric vehicle before a dishwasher or an air conditioner can start operation.

Modeling the inter-dependencies among industrial units is challenging. There are several factors that must be considered. For example, in some cases, the operation of a unit that is being fed must start immediately after the feeding unit finishes its operation. This may be the case when the feeding unit’s output has to be used as soon as it reaches a certain pressure or temperature. Furthermore, the operation of some industrial units, e.g., in chemical industries, cannot be interrupted. Yet, there are units, e.g., in the automotive industry, that can be interrupted and later restored. While some of these aspects are briefly discussed, e.g., in [6] and [7], there is still a need to develop a more comprehensive framework for industrial load control that can support different types of industrial units.

In this paper, we propose an optimization-based approach to industrial load control. To gain insight, we discuss a case study of oil refineries which are among the most energy intensive industries in the United States and around the world. In fact, it is estimated that the oil refineries in the United States purchased 46,195 MWh electricity in 2011 [8]. Our proposed optimization model is comprehensive and takes into consideration the day-ahead electricity price, operation completion constraints, sequential operation constraints, immediate start constraints, uninterruptable operation constraints, and maximum load constraints. The formulated problem is a tractable linear binary program and results in noticeably reducing the electricity cost of the oil refinery in the case study.

The rest of this paper is organized as follows: An overview of the oil refinery industry and its operational requirements are discussed in Section II. Optimization-based industrial load control is proposed in Section III. Numerical results are given in Section IV. The paper is concluded in Section V.

II. OIL REFINERY INDUSTRY

A. Background

In this section, we provide a brief overview of a typical crude oil processing facility, based on the example of the BP Kwinana refinery [9]. The flow diagram of the processes is shown in Fig. 1. Crude oil, which is a combination of various hydrocarbons, is first distilled in the Crude Distillation Unit, where it is divided into a number of fractions including gas, naphtha, kerosene, gas oil, and residue. The Amine and Merox

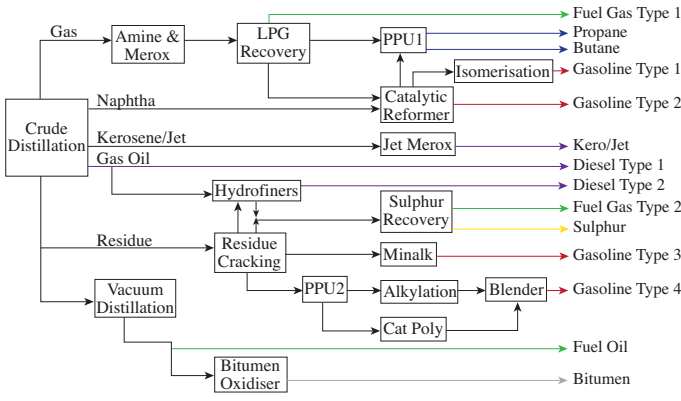


Fig. 1. Flow diagram of crude oil processing at the BP Kwinana Oil Refinery with 17 processing units and 14 different final products [9].

unit then removes hydrogen sulfide and/or mercaptans from gas. In the LPG Recovery Unit, liquid petroleum gas (LPG) is recovered. The Catalytic Reformer further processes the naphtha and gasoline that come from the Crude Distillation Unit to make them suitable components for blending into motor spirit. LPG is fed to the Propane Production Unit 1 (PPU1) for separation into propane and butane. The Isomerisation Unit uses a process designed to upgrade the octane number of Light Hydrotreated Naphtha from the Catalytic Reformer. The Jet Merox Unit takes Jet from the Crude Distillation Unit and removes the mercaptans. The Residue Cracking Unit breaks down the long chain hydrocarbons into smaller, more valuable components. The Hydrofiners enable the refinery to process sour crude, which has higher sulphur content. Hydrofiner takes Light Cycle Oil from the Residue Cracking Unit and both take gas oil from the Crude Distillation Unit. Sulphur is removed through a hydrotreating process, and the result is the sweetened oil that is blended to make diesel. The Sulphur Recovery Unit removes sulphur from gas streams that could otherwise contribute to atmospheric emissions. The PPU2 takes LPG from the Residue Cracking Unit and removes hydrogen sulphide and mercaptan sulphur. The mixed LPG is then split into C3 and C4 streams. The C3 stream can be sold directly or be passed to the Catalytic Polymerisation Unit (CPU) for further processing. The bulk of the C4 stream goes to the Alkylation Unit, while the remainder goes to the CPU. The Alkylation unit combines smaller molecules to produce high-octane motor spirit. Vacuum Distillation Unit distills the residue further. Finally, Bitumen is made from the heavy ends of crude oil by the Vacuum Distillation Unit [9].

B. Directed Graph Representation

In this section, we provide a *directed acyclic graph representation* of the inter-connecting units inside an industrial complex. Our focus is again on the example of an oil refinery. The directed graph representation of the inter-connecting units in the BP Kwinana Refinery is shown in Fig. 2. In total, there are 18 nodes in this graph. Nodes 1 to 17 represent the processing units in the following order: Crude Distillation, Amine & Merox, LPG Recovery, Catalytic Reformer, PPU1, Isomerisation, Jet Merox, Residue Cracker, Minalk, Hydrofiners, Sulphur Recovery, PPU2, Alkylation, Cat Poly, Blender, and Bitumen Oxidiser.

The last (i.e., the 18th) node is labeled as Final Products and represents the unit that collects and exports the final products.

The graph edges indicate the presence and type of inter-dependencies among the units. In particular, the directed edge (i, j) from node i to node j indicates that node i is a feeding unit of node j ; therefore, node j may start operation only if the operation of node i is finished. For each edge (i, j) , the weight $a_{i,j}$ indicates the time (in terms of 15 minutes time slots) that it will take for unit i to finish its operation¹. As an example, consider edge $(4, 6)$ with weight $a_{4,6} = 3$. This indicates that unit 6 may not start operation until unit 4 finishes its operation. It also indicates that it will take 3 time slots, i.e., $3 \times 15 = 45$ minutes for unit 4 for finish its operation. Also note that some nodes may have multiple incoming edges. For example, node 15 has an incoming edge from node 13 and another incoming edge from node 14. This is because both units 13 and 14 are feeding units for unit 15.

The directed graph representation in Fig. 2 can explain the sequence of processes that lead to each final product. For example, to produce Fuel Gas Type 1, the following operational sequence can be identified. First, unit 1 should operate for $2 \times 15 = 30$ minutes. Then, unit 2 should operate for $1 \times 15 = 15$ minutes. After that, unit 3 should operate for $2 \times 15 = 30$ minutes. Hence, from the moment that unit 1 starts its operation, it will take at least $(2+1+2) \times 15 = 75$ minutes before Fuel Gas Type 1 can be ready. Similar operational sequences can be identified for other final products.

Each edge can be either a solid line or dashed line, based on the type of dependencies among units. Solid edges indicate the requirement for immediate start, while dashed edges indicate the flexibility for a delayed start. For example, consider the solid edge $(8, 9)$. It indicates that the operation of unit 9 must start immediately after the operation of unit 8 is complete. In contrast, the dashed edge $(2, 3)$ indicates that the operation of unit 3 can be started any time (i.e., with delay, if needed) after the operation of unit 2 is complete.

Each node can be represented by either a circle or a square. Circle nodes are interruptable units. For example, consider unit 12, which has outgoing edges with weight 2. The operation of this unit is complete after $2 \times 15 = 30$ minutes, whether it is a consecutive 30 minutes or two separate 15 minutes. In contrast, square nodes are uninterruptable units which are less flexible. For example, consider unit 8, which has outgoing edges with weight 4. The operation of this unit is complete after $4 \times 15 = 60$ minutes. However, since unit 8 is uninterruptable, it may only operate in a consecutive 60 minutes. That is, it cannot operate at four separate 15 minutes or two separate 30 minutes. Once an uninterruptable unit starts operation it cannot be switched off until it finishes its operation.

Finally, there is a per-time slot electricity consumption associated with each unit. For example, the per-time slot electricity consumption associated with unit 8 is 16 kWh. Since the operation of unit 8 is completed in 4 times lots, the total electricity consumption of unit 8 to finish operation is

¹The edge weights include hold-up times, i.e., the time required to transport the processed materials from one unit to the next. It is assumed that electricity consumption of a unit remains the same during the hold-up time.

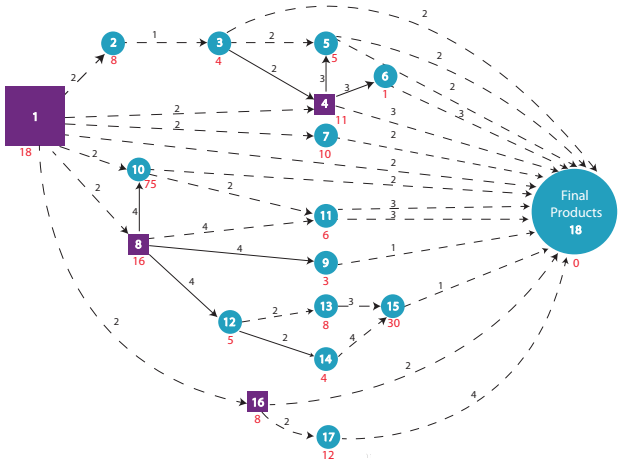


Fig. 2. Directed graph representation of the flow diagram in Fig. 1.

$4 \times 16 = 64$ kWh. Of course, since unit 8 is an uninterruptable unit, it must consume 64 kWh in a single one-hour period.

Note that in [9], BP did not release enough information to allow us set the numbers for weights of edges, weights of nodes, types of edges, and types of nodes according to BP's actual facility. However, for the purpose of demonstration, some data shown in Fig. 2 are collected and scaled from other sources including [10], and the rest are chosen randomly.

C. Potential for Load Control

To gain insight about the potential for designing an industrial load control for the processes in the oil refinery described in Figs. 1 and 2, consider the two energy consumption scheduling examples in Fig. 3. Both schedules are acceptable in the sense that they both satisfy the operational requirements that we described in Section II-B. However, if the price of electricity is not flat, then the electricity cost of implementing these two energy consumption schedules can be very different. In fact, for the sample day-ahead electricity prices shown in the second to last row in Figs. 3(a) and (b), the electricity cost of the first schedule becomes \$26.5, while the electricity cost of the second schedule becomes \$16.1, i.e., 40% less. These simple examples show that there is a great potential to reduce the energy expenditure of this case study if appropriate load control is implemented.

III. OPTIMAL INDUSTRY LOAD CONTROL

In this section, we formulate an optimization problem for industrial load control. Let $\mathcal{V} = \mathcal{S} \cup \mathcal{C}$ and $\mathcal{E} = \mathcal{D} \cup \mathcal{I}$ denote the set of all nodes and the set of all edges in the graph representation of the industrial complex of interest, respectively. Here, \mathcal{S} is the set of square nodes and \mathcal{C} denotes the set of circle nodes. Furthermore, \mathcal{D} is the set of edges that are represented with dashed lines and \mathcal{I} denotes the set of edges that are represented by solid lines. Time is divided into equal length time slots. Without loss of generality, we assume that the length of each time slot is 15 minutes. The set of time slots is denoted by $\mathcal{T} = \{1, \dots, M\}$, where M is the number of time slots in the scheduling horizon. For example,

Unit \ T.S.	1	2	3	4	5	6	7	8	9	10	11	12	13	14	15	16	17	18	19	20	
1	1																				
2		1																			
3			1																		
4				1																	
5					1																
6						1															
7							1														
8								1													
9									1												
10										1											
11											1										
12												1									
13													1								
14														1							
15															1						
16																1					
17																	1				
18	18	18	8	4	8	8	16	16	16	32	106	113	51	24	4	18	30	5	1	1	497
Price	0.02	0.02	0.02	0.03	0.03	0.03	0.04	0.04	0.04	0.06	0.06	0.07	0.06	0.05	0.04	0.05	0.04	0.03	0.03	0.03	26.5
Cost	0.39	0.45	0.2	0.11	0.23	0.25	0.57	0.59	0.71	1.76	6.5	7.84	3.26	1.2	0.17	0.85	1.17	0.17	0.03	0.03	26.5

(a)

Unit \ T.S.	1	2	3	4	5	6	7	8	9	10	11	12	13	14	15	16	17	18	19	20	
1	1																				
2		1																			
3			1																		
4				1																	
5					1																
6						1															
7							1														
8								1													
9									1												
10										1											
11											1										
12												1									
13													1								
14														1							
15															1						
16																1					
17																	1				
18	18	18	42	28	32	39	94	86	6	5	4	1	1	4	4	4	8	14	26	63	497
Price	0.02	0.02	0.02	0.03	0.03	0.03	0.04	0.04	0.04	0.06	0.06	0.07	0.06	0.05	0.04	0.05	0.04	0.03	0.03	0.03	16.1
Cost	0.39	0.45	1.04	0.8	0.94	1.24	3.38	3.17	0.27	0.28	0.25	0.07	0.06	0.2	0.17	0.19	0.31	0.46	0.78	1.61	16.1

(b)

Fig. 3. Two example energy consumption schedules to implement the flow diagram of Fig. 1. While both schedules are acceptable, the electricity cost of implementing the schedule in (b) is significantly less than that of in (a).

in case of day-ahead energy consumption scheduling, we have $M = 24 \times 4 = 96$. The per-time slot electricity consumption associated with each node i is denoted by l_i .

A. Decision Variables

For each unit $i \in \mathcal{V}$, let $x_i(t) \in \{0, 1\}$ denote whether unit i is operating during time slot $t \in \mathcal{T}$. That is, we have $x_i(t) = 1$ if unit i is 'on' during time slot t and $x_i(t) = 0$ if unit i is 'off' during time slot t . The decision variables in our proposed optimal industrial load control framework are $\mathbf{x} = (x_i(t), \forall i \in \mathcal{V}, t \in \mathcal{T})$.

B. Objective Function

At each time slot $t \in \mathcal{T}$, the total scheduled electricity consumption of the industrial complex can be calculated as

$$\sum_{i \in \mathcal{V}} x_i(t) l_i. \quad (1)$$

Thus, the electricity cost of the complex in the scheduling horizon becomes

$$\sum_{t \in \mathcal{T}} \left(\sum_{i \in \mathcal{V}} x_i(t) l_i \right) p(t), \quad (2)$$

where $p(t)$ denotes the price of electricity at time slot t . The objective in our proposed optimal industrial load control framework is to minimize the expression (2).

C. Operation Completion Constraints

To assure completion of the operation of all units within the scheduling horizon, for each unit $i \in \mathcal{V}$, it is required that

$$\sum_{t \in \mathcal{T}} x_i(t) = a_i, \quad (3)$$

where $a_i = a_{i,j}$ for each $(i,j) \in \mathcal{E}$. Note that we assume all outgoing edges of each unit in the graph representation have the same weight, as is shown in Fig. 2.

D. Sequential Operation Constraints

Due to the inter-dependency among units, a particular unit cannot start its operation until all units that feed it finish their operations. This can be modeled mathematically if for each pair of nodes $i, j \in \mathcal{V}$ such that $(i,j) \in \mathcal{E}$, we have

$$x_j(t) \leq \frac{1}{a_{i,j}} \sum_{k=1}^{t-1} x_i(k), \quad \forall t \in \mathcal{T}. \quad (4)$$

From (4), if $\sum_{k=1}^{t-1} x_i(k) < a_{i,j}$, i.e., if the operation of unit i is *not* completed before time slot t , then $x_j(t) = 0$, i.e., unit j *cannot* start its operation at time slot t . Together, constraints (4) for all $(i,j) \in \mathcal{E}$ will assure that the operation of unit j may start only after all its feeding units finish their operation.

E. Immediate Start Constraints

Recall from Section II-B that if an edge (i,j) is shown as a solid line in the graph representation in Fig. 2, then it indicates that the operation of unit j must start immediately after unit i finishes its operation. This can be modeled mathematically if for each pair of nodes $i, j \in \mathcal{V}$ such that $(i,j) \in \mathcal{I}$, we have

$$x_j(t) \leq x_i(t-1) + \sum_{k=1}^{t-1} x_j(k), \quad \forall t \in \mathcal{T} \setminus \{1\}. \quad (5)$$

From (5), at each time slot $t \in \mathcal{T}$, $x_j(t)$ is nonzero only if either $\sum_{k=1}^{t-1} x_j(k) > 0$, i.e., the operation of unit j has already started, or $x_i(t-1) = 1$, i.e. unit i was operating during the last time slot. Together, constraints (3)-(5) assure that unit j starts operation as soon as the operation of unit i is complete.

F. Uninterruptible Operation Constraints

Recall that uninterruptible units are presented as square nodes in the graph representation in Fig. 2. For an uninterruptible unit, once the operation starts, it must continue until the operation is completed. This property can be modeled mathematically if for each node $i \in \mathcal{S}$, we have

$$x_i(t) \leq x_i(t+1) + \frac{1}{a_i} \sum_{k=1}^t x_i(k), \quad \forall t \in \mathcal{T} \setminus \{M\}. \quad (6)$$

where a_i is defined in Section III-C and denotes number of time slots that unit i should operate. From (6), at each time slot $t \in \mathcal{T}$, $x_i(t)$ is nonzero only if either $x_i(t+1) = 1$, i.e., the operation of unit i continues in the next time slot, or $\sum_{k=1}^t x_i(k) = a_i$, i.e., the operation of unit i finishes by the end of the current time slot. It is worth mentioning that constraint (6) is different from a partly similar constraint that was defined for uninterruptible loads in [2]. In particular, it does *not* require using any auxiliary variable.

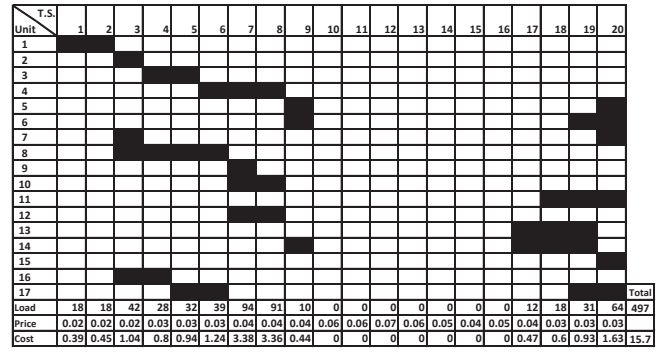


Fig. 4. Optimal energy consumption schedule based on the proposed scheme.

G. Maximum Load Constraint

The total power draw of the industrial complex of interest should also be maintained below a limit at any time:

$$\sum_{i \in \mathcal{V}} l_i x_i(t) \leq L_{\max}, \quad \forall t \in \mathcal{T}, \quad (7)$$

where $L_{\max} > 0$ is set by the utility and depends on the limits of the power grid and the transmission lines in the region.

H. Optimization Problem Formulation

An optimal industrial load control can be modeled as the solution of the following optimization problem:

$$\begin{aligned} & \text{Minimize}_x \quad \sum_{t \in \mathcal{T}} \left(\sum_{i \in \mathcal{V}} x_i(t) l_i \right) p(t) \\ & \text{Subject To} \quad (3) - (7). \end{aligned} \quad (8)$$

It is a *linear binary program* which can be solved using optimization software, such as MOSEK [11] and CPLEX [12].

IV. NUMERICAL RESULTS

In this section, we assess our proposed industrial load control scheme for the BP refinery in Kwinana in Figs. 1 and 2. The number of time slots in the scheduling horizon is $M = 20$, i.e. the decision horizon is five hours. The limit on total load at each time slot is $L_{\max} = 300 \text{ kWh}$.

A. Optimal Schedule

The optimal load schedule is shown in Fig. 4. It is calculated based on the solution of problem (8). We can see that although optimal scheduling consumes the same amount of electricity during scheduling horizon as the two examples of Section II-C, it results in noticeably lower electricity cost.

Next, we repeat the analysis for 100 different pricing scenarios, based on the day-ahead price profiles in [13]. The results are shown in Fig. 5, where we compare our optimal load control approach with a base method that schedules the operation of each unit with no interruption and as soon as all its feeding units finish their operations. At every pricing scenario, our optimal scheduling cost is lower. On average, optimal load control can reduce the cost by over 14%.

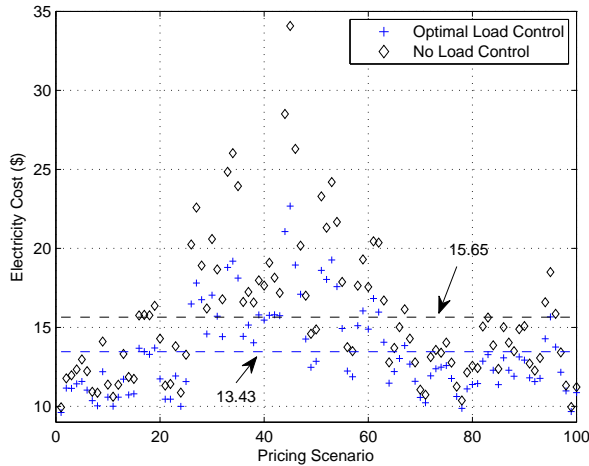


Fig. 5. Reducing electricity cost via optimal load control for 100 different price scenarios.

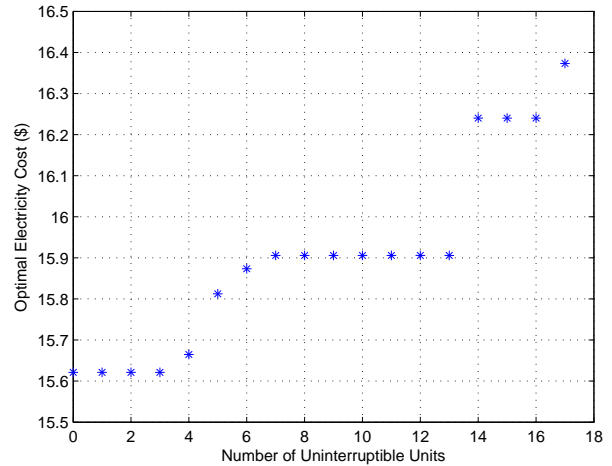


Fig. 7. The impact of number of uninterruptible units on optimal cost

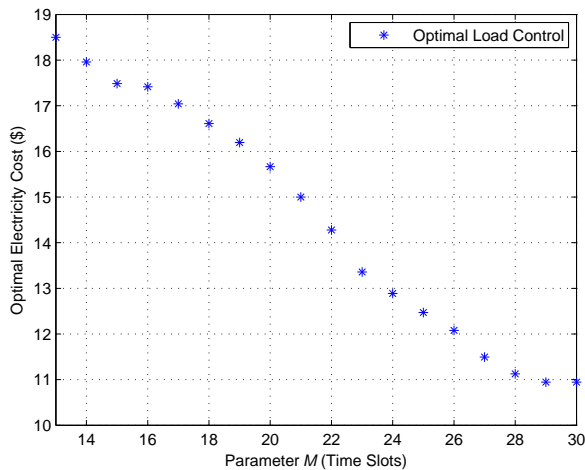


Fig. 6. The impact of parameter M on optimal electricity cost.

B. Changing the Decision Horizon

The impact of changing parameter M on electricity cost is shown in Fig. 6. We can see that the optimal cost decreases or does not change as M increases. This is because a higher M indicates more time flexibility. Note that parameter M is lower bounded by 13 time slots, which is the minimum number of time slots required to finish the operation of all units.

C. Units Types and Edges Types

In general, interruptable units (i.e., circle nodes) and non-immediate dependencies (i.e., dashed lines) cause more flexibility in load scheduling and consequently lower electricity cost. An example is shown in Fig. 7. We can see that, as we increase the number of uninterruptable units (and accordingly decrease the number of interruptable units), problem (8) will face more restrictive constraints that may lead to increasing the electricity cost associated with the industrial complex.

V. CONCLUSIONS AND FUTURE WORK

Since a big portion of the generated electricity is consumed by the industrial sector, optimal load control can significantly help industrial complexes to cut their electricity expenditure. To gain insight, we considered the example of an oil refinery and proposed a mathematical framework to conduct optimal load control. Simulation results showed that by scheduling the load in accordance with the day-ahead pricing profiles, we can significantly reduce electricity bills for industrial units.

The future plan is to improve formulation by considering multiple operation modes instead of on-off, considering ramping of industrial units, and considering storage limitation.

REFERENCES

- [1] "International energy outlook 2011," Tech. Rep. DOE/EIA-0484(2011), Sep. 2011. [Online]. Available: <http://www.eia.gov/forecasts/ieo>
- [2] A. H. Mohsenian-Rad and A. Leon-Garcia, "Optimal residential load control with price prediction in real-time electricity pricing environments," *IEEE Trans. on Smart Grid*, vol. 1, no. 2, pp. 120–133, 2010.
- [3] Y. Guo, M. Pan, and Y. Fang, "Optimal power management of residential customers in the smart grid," *IEEE Trans. on Parallel & Distributed Systems*, vol. 23, no. 9, pp. 1593–1606, 2012.
- [4] M. A. P. S. Kiliccote and D. Hansen, "Advanced controls and communications for demand response and energy efficiency in commercial buildings," *Proceedings of Second Carnegie Mellon Conference in Electric Power Systems*, Jan. 2006.
- [5] "Key world energy statistics 2012," International Energy Agency, Tech. Rep., 2012. [Online]. Available: <http://www.iea.org/publications/freepublications/publication/kwes-1.pdf>
- [6] S. Ashok and R. Banerjee, "An optimization mode for industrial load management," *IEEE Trans. on Power Systems*, vol. 16, no. 4, pp. 879–884, Nov. 2001.
- [7] C. A. Babu and S. Ashok, "Peak load management in electrolytic process industries," *IEEE Trans. on Power Systems*, vol. 23, no. 2, pp. 399–405, May 2008.
- [8] "Refinery capacity report," Energy Information Administration, Tech. Rep. Form EIA-820, "Annual Refinery Report", Jun. 2012. [Online]. Available: <http://www.eia.gov/petroleum/refinerycapacity/table10.pdf>
- [9] "BP kwinana refinery- public environmental report," Tech. Rep., Jan. 2011. [Online]. Available: <http://tinyurl.com/PER-BP-Kwinana-2009>
- [10] E. Worrell and C. Galitsky, "An ENERGY STAR guide for energy and plant managers," Tech. Rep., 2005.
- [11] "MOSEK Optimization Software," <http://www.mosek.com/>.
- [12] "IBM CPLEX Optimization Software," <http://www-01.ibm.com/software/integration/optimization/cplex-optimizer/>.
- [13] <https://www2.ameren.com/RetailEnergy/realtimeprices.aspx>.